Letter

Effective Luttinger parameter and Kane-Fisher effect in quasiperiodic systems

T. J. Vongkovit,[1] Hansveer Singh,[2] Romain Vasseur,[2] and Sarang Gopalakrishnan[1]
[1]*Department of Electrical and Computer Engineering, Princeton University, Princeton, New Jersey 08544, USA*
[2]*Department of Physics, University of Massachusetts, Amherst, Massachusetts 01033, USA*

(Received 8 April 2024; revised 24 May 2024; accepted 18 June 2024; published 12 July 2024)

The ground states of interacting one-dimensional metals are generically Luttinger liquids. Luttinger-liquid theory is usually considered for translation invariant systems. The Luttinger-liquid description remains valid for weak quasiperiodic modulations; however, as the quasiperiodic modulation gets increasingly strong, it is increasingly renormalized and eventually fails, as the system becomes localized. We explore how quasiperiodic modulation renormalizes the Luttinger parameter characterizing this emergent Luttinger liquid, using the renormalization of transmission coefficients across a barrier as a proxy that remains valid for general quasiperiodic modulation. We find, unexpectedly, that quasiperiodic modulation weakens the effects of short-range interactions, but enhances those of long-range interactions. We support the former finding with matrix-product numerics. We also discuss how interactions affect the localization phase boundary.

DOI: 10.1103/PhysRevB.110.L020201

Introduction. The nature of ground-state correlations in interacting disordered systems has been a question of long-standing interest [1–4]. In one dimension, this question has been addressed from two complementary perspectives: perturbatively adding disorder to clean interacting systems [5], and perturbing the disordered system with weak interactions using the strong disorder renormalization group (SDRG) [6]. These approaches agree in finding two phases—a localized insulating phase and a Luttinger-liquid phase—but give contrasting predictions for the critical behavior between them (see also Refs. [7–9]). In many present-day experiments, the spatial modulations are quasiperiodic rather than random: both in cold-atom experiments using incommensurate potentials [10–15] and more recently in moiré materials [16,17]. Quasiperiodic systems exhibit many of the same phenomena as random ones, e.g., Anderson localization, but their properties are fundamentally different because of the deterministic, hyperuniform structure of quasiperiodic patterns [18–21]. Quasiperiodic systems present distinctive theoretical challenges, as many of the methods used in the random case (such as the replica trick) are no longer useful.

In the absence of controlled analytical methods, progress on understanding the ground-state properties of interacting quasiperiodic systems has come from a combination of numerical [22–32] and perturbative approaches. As in the random case, the two complementary perturbative approaches are to treat interactions nonperturbatively in the Luttinger-liquid framework, but perturb in disorder [22], or to begin with the scaling theory of the noninteracting critical point, and perturb in interactions, as in very recent work [31]. These approaches yield distinct universality classes for the localization transition: In the former case, the transition is Lorentz invariant; in the latter, the Luttinger liquid never emerges and the localization transition remains in the noninteracting universality class. To reconcile these pictures it is imperative to understand how Luttinger-liquid behavior emerges (or fails to emerge) for strong quasiperiodic modulation, and how Luttinger-liquid properties evolve with quasiperiodicity. We address these questions, focusing on interacting spinless fermions with finite-range interactions. (The spinful case was recently explored [33].)

Increasing the quasiperiodic potential strength causes the single-particle bands to get increasingly flat [34]. As flat bands are associated with enhanced interactions, so one might expect a quasiperiodic potential to strengthen interaction effects. Surprisingly, this is not the case in general; instead, the *range* of the interactions plays a crucial part. For short-range interactions, the quasiperiodic potential suppresses interactions and make the system more free-fermion-like [31]. On the other hand, long-range interactions are enhanced by the quasiperiodic potential. We establish these results by two distinct means. First, we perform density matrix renormalization group (DMRG) simulations of one-dimensional quasiperiodic spin chains [35,36] and extract the Luttinger parameter, which quantifies interaction strength. Second, we study the renormalization of transmission through a barrier, adapting the treatment of Yue *et al.* [37] to the quasiperiodic case. The renormalization of the transmission coefficient gives us a way of extracting an effective Luttinger parameter from Hartree-Fock studies.

Model. We will focus on a single-band model of spinless fermions, interacting with finite-range interactions, governed by the Hamiltonian

$$H = \sum_i \{c_i^\dagger c_{i+1} + \text{H.c.} + \lambda \cos[\varphi(i+\theta)] n_i\} + \sum_{ij} V_{ij} n_i n_j, \tag{1}$$

where φ is the golden ratio, c_i annihilates a fermion on site i and $n_i \equiv c_i^\dagger c_i$, and the overall energy scale has been set to unity. We briefly review the properties of this model in the noninteracting case $V_{ij} = 0$. This is the familiar Aubry-André (AA) model. When $\lambda < 2$ the single-particle eigenstates of this model are delocalized and ballistic; for $\lambda > 2$ all

single-particle states are localized. Unusually, the localization transition occurs at the same value of λ for all states in the spectrum. At the critical value $\lambda = 2$, not only are all the eigenstates localized, but the *spectrum* is highly unusual: All the single-particle eigenvalues are in a fractal, measure-zero set, so the bands are anomalously flat [38,39]. For $\lambda < 2$ as one approaches the critical point, the spectrum consists of many increasingly flat minibands. The conventional wisdom is that these flat minibands will tend to make the system highly susceptible to interactions.

We consider two choices for the interactions V_{ij}. First, for our exact numerical studies, we take the interactions to be nearest neighbor, i.e., $V_{ij} = \Delta\delta_{i,j\pm1}$. The nearest-neighbor model is appealing for numerical studies because it can be mapped via a Jordan-Wigner transformation to a canonical nearest-neighbor spin model, the anisotropic Heisenberg model. This allows for efficient DMRG simulations, and also allows us to compare our numerical results in the clean limit with exact results in the literature. However, as we will see, the range of the interaction plays an important part in the physics of the model. To allow us to tune this range d, we will also consider interactions that decay with a Gaussian envelope:

$$V_{\text{int}}(|i-j|) = \frac{v_{\text{int}}}{d\sqrt{\pi}} \exp\left[-(i-j)^2/d^2\right]. \tag{2}$$

Long-range interactions can be naturally incorporated in our Hartree-Fock analysis. They are possible [40] but potentially challenging to treat in DMRG. We note that the Hartree-Fock method has other advantages, as it allows us to address aspects of the dynamics (and disentangle distinct physical effects) in a way that would not be possible with DMRG.

When $\lambda < 2$, at a typical filling the Fermi level lies inside a miniband. One can treat sufficiently weak interactions by linearizing the single-particle spectrum about the Fermi level and treating the interactions projected onto a single miniband. This yields a Luttinger liquid, in which the strength of correlations is set by the Luttinger parameter K (defined below). Linearizing becomes an increasingly inaccurate approximation as one approaches $\lambda = 2$: Any finite interaction strength mixes many minibands. Nevertheless, we find that the effect of the other minibands manifests itself as a finite renormalization of the Luttinger parameter, without changing the asymptotic nature of correlations.

One can understand our main results intuitively by thinking about the behavior of interactions projected onto a single miniband. The well-defined minibands at some $\lambda < 2$ are essentially the Bloch bands of a periodic approximant with denominator q to the true incommensurate potential. As q grows, the minibands split, so the Bloch states of each miniband are made up of increasingly well-separated ($\sim q$) Wannier states. For any finite interaction range d, eventually $q \gg d$, so the interactions projected onto the miniband are contact-like. A contact interaction has no effect on identical spinless fermions, so the projected problem becomes noninteracting. This accounts for the surprising robustness of the flat minibands of the Aubry-André model to interactions.

DMRG results. We begin by extracting the Luttinger parameter directly from DMRG calculations on the ground state of the quasiperiodically modulated problem at half filling. Our primary diagnostic for the Luttinger parameter is the

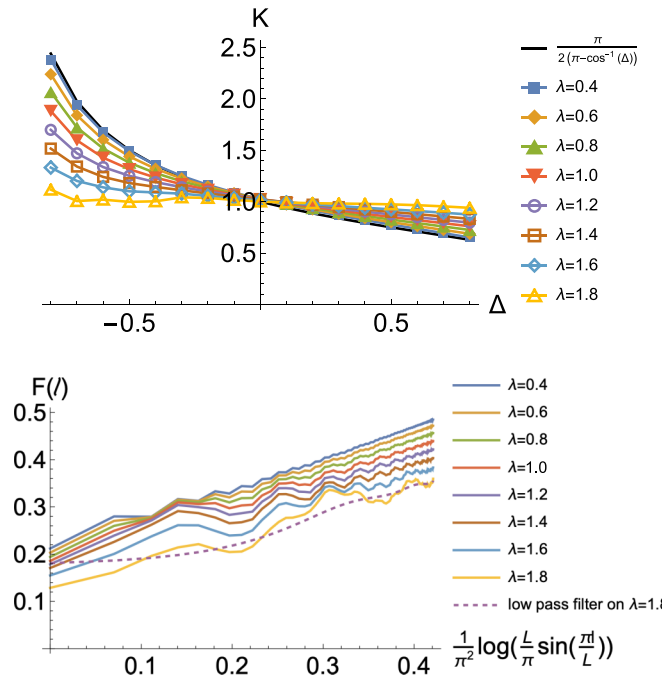

FIG. 1. Upper panel: Luttinger parameter K extracted from subsystem charge fluctuations, as a function of the interaction strength Δ, for various values of the quasiperiodic potential strength λ. At $\lambda = 0$ there is a known analytic value, plotted as a solid line [41]. Note that as λ is increased the curves get increasingly flat, at the noninteracting value $K = 1$. Lower panel: Dependence of charge fluctuations on subsystem size for interactions $\Delta = -0.5$ and various values of λ. At higher values of λ stronger oscillations appear, so we thus feed the data through a low pass filter (using 0.1 for the cutoff frequency) in order to smooth out oscillations and then perform a linear fit. DMRG simulations were done with $L = 200$ and a maximum bond dimension of 200. Data are averaged over 20 phase realizations.

variance of the charge in a half system, i.e., the behavior of the following connected correlation function for a subsystem of length ℓ,

$$F(\ell) = \left\langle \left(\sum_{i=1}^{\ell} n_i \right)^2 \right\rangle - \left\langle \left(\sum_{i=1}^{\ell} n_i \right) \right\rangle^2, \tag{3}$$

where expectation values are taken in the ground state. In a Luttinger liquid with open boundary conditions in a system of size L, one expects $F(\ell) = \frac{K}{2\pi^2} \log[\frac{L}{\pi} \sin(\frac{\pi\ell}{L})]d$, where K is the Luttinger parameter [41].

The results for the charge fluctuations are shown in Fig. 1. The charge fluctuations are logarithmic in ℓ, as expected for a Luttinger liquid. Extracting K from the coefficient of the logarithm, we find that $K \to 1$—the noninteracting value—as λ is increased at fixed interaction strength Δ. As one might expect, the onset of the clear logarithmic scaling regime is pushed out to larger ℓ as we increase λ. In the Supplemental Material [42] we also consider a separate diagnostic, namely the two-point correlator of the "spins" related to the fermions of Eq. (1) by a Jordan-Wigner transformation. This diagnostic is *a priori* unrelated to the charge fluctuations, but in a Luttinger liquid, these two observables are tightly related. Consistent estimates

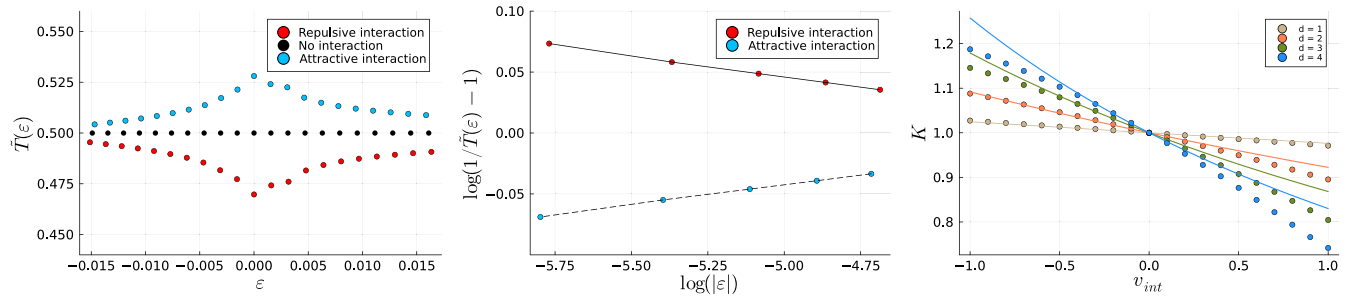

FIG. 2. Data on transmission coefficients in the clean system, computed for system size $N = 2501$ and filling fraction $f = 0.1$. Left: Transmission coefficient as a function of energy measured from the Fermi level, for $v_{\text{int}} = \pm 0.6$ and without interactions. Middle: Same data but on a log-log plot, showing the nonanalytic behavior of the transmission coefficient near E_F. Right: Exponent $\tilde{\alpha}$ (dots) compared with the continuum analytic prediction α [Eq. (5)], as a function of interaction strength, for various choices of the interaction range. Discrepancies at larger interaction strengths are expected as lattice dispersion effects become significant.

of K from these two approaches are a consistency check that the system is a Luttinger liquid.

These numerical observations lead to the conclusions that (1) the system is a Luttinger liquid throughout the delocalized phase of the Aubry-André model, and (2) the Luttinger parameter is renormalized toward its noninteracting value as the quasiperiodic potential is increased. These observations are consistent with the qualitative picture presented in the preceding section.

Kane-Fisher effect: Self-consistent approach. The previous section presented numerically exact calculations for the case of nearest-neighbor interactions. We now turn to an approximate but versatile approach that sheds light on the mechanism for Luttinger-parameter suppression, and also lets us extend our analysis to models with tunable-range interactions. In this section we introduce the basic idea behind the method for clean systems; the next section applies the method to quasiperiodic systems.

The basic tool we will use to diagnose correlations is the Kane-Fisher effect [43], i.e., the renormalization of tunneling across a localized impurity due to interactions. At zero temperature and at incident energies E close to the Fermi energy E_F, the renormalized transmission coefficient across the impurity scales as $T(E) \sim |E - E_F|^{2(K^{-1}-1)}$. Thus, tunneling is parametrically suppressed (enhanced) for repulsive (attractive) interactions. Although the Kane-Fisher effect is normally studied using bosonization techniques that do not generalize to our setting, there is an alternative weak-coupling formulation due to Yue *et al.* [37] that is more versatile. In this treatment, one begins with the observation that a static impurity in a Fermi gas creates Friedel oscillations in the density profile of the surrounding gas. These Friedel oscillations renormalize the effective scattering shift experienced by electrons farther away from the impurity, thus further renormalizing the Friedel oscillations, and so forth. Solving self-consistently for the tunneling across the impurity one recovers the Kane-Fisher effect.

To explore the effect of quasiperiodic modulations on the Kane-Fisher effect, we first self-consistently solve for the ground state in the presence of the impurity, in the Hartree-Fock approximation, and then numerically solve for tunneling across the impurity. It might seem surprising that a mean-field approximation such as Hartree-Fock can capture a correlation-dominated quantity such as the Luttinger parameter. Intuitively, the reason why this is possible is that the way the electrons avoid the impurity in the mean-field treatment is essentially analogous to the way they avoid each other due to correlations. In any case, we note that the predicted power-law divergences are clearly seen in the self-consistent Hartree-Fock numerical solution (Fig. 2).

Before turning to our numerical results, we briefly summarize the main results of Ref. [37]. This work linearizes the dispersion around the Fermi surface, projecting to states with energies within $D_0 = v_F/d$ of E_F. Solving self-consistently for the potential [42] gives the result for the transmission coefficient [37]

$$T(\epsilon) = \frac{T_0|\epsilon/D_0|^{2\alpha}}{R_0 + T_0|\epsilon/D_0|^{2\alpha}}, \tag{4}$$

where $\epsilon = E - E_F$ and $T_0 = |t_0|^2$ and $R_0 = 1 - T_0$ are the bare transmission and reflection coefficients. The dimensionless parameter α is defined by [37]

$$\alpha = \alpha_{\text{exchange}} - \alpha_{\text{Hartree}},$$
$$\alpha_{\text{exchange}} = \frac{\tilde{V}(0)}{2\pi v_F}, \quad \alpha_{\text{Hartree}} = \frac{\tilde{V}(2k_F)}{2\pi v_F}. \tag{5}$$

Here, $\alpha = K^{-1} - 1$. In the continuum limit, the exchange and Hartree terms have opposite effects on the transmission coefficient. In the case of a repulsive (attractive) interaction, the exchange term decreases (increases) the transmission coefficient compared to its bare value, while the Hartree term increases (decreases) it. For zero-range interactions, the exchange and Hartree terms cancel exactly, as they must because contact interactions have no effect on spinless fermions.

We now describe our numerical method for calculating transmission coefficients on the lattice, focusing first on the case without a quasiperiodic potential. We will work with Eq. (1) with a finite-range Gaussian interaction Eq. (2). We perform a mean-field Hartree-Fock decoupling of the interaction term, $V_{\text{int}}(i,j)n_i n_j \approx V_H(i)c_i^\dagger c_i + \sum_{i\neq j} V_{\text{ex}}(i,j)c_i^\dagger c_j$, where $V_H(i) = \sum_{j\neq i} V_{\text{int}}(|i-j|)\langle c_j^\dagger c_j\rangle$ and $V_{\text{ex}}(i,j) = -V_{\text{int}}(|i-j|)\langle c_j^\dagger c_i\rangle$.

To compute the transmission coefficient we proceed as follows. First, we solve the Hartree-Fock problem fully self-consistently for the ground state. Next, we treat the dynamics

of wave-packet transmission under this self-consistent quadratic Hamiltonian. In the clean case, the transmission coefficient can be computed using scattering theory. Once the quasiperiodic potential is turned on, we do not have a simple expression for the asymptotic states. Therefore, to calculate the transmission coefficient, we construct a wave packet localized in real space to one side of the barrier, and sharply localized in energy space at some energy E displaced by ϵ from E_F. We allow the wave packet to evolve in time and scatter off the barrier, defining the transmission coefficient $\tilde{T}(\epsilon)$ as the modulus squared of the portion of the wave packet that passes through the barrier to the other side.

Our results for the clean case are summarized in Fig. 2. To minimize lattice effects we work at a filling $f = 0.1$. The left panel shows the transmission coefficient as a function of energy (measured with reference to E_F), showing a dip (peak) for repulsive (attractive) interactions. Note that in the noninteracting case the transmission coefficient is smooth across E_F. The middle panel of Fig. 2 shows that the transmission diverges/vanishes as a power law, consistent with Eq. (4). From this power-law dependence one can extract a numerical exponent $\tilde{\alpha}$. This is shown in the right panel of Fig. 2. In the thermodynamic limit, for weak enough interactions and low enough filling, we expect that the numerical value $\tilde{\alpha}$ should approach the continuum analytic value of α (5). Our data are consistent with this. For stronger interactions, it is no longer quantitatively accurate to linearize the lattice dispersion around the Fermi surface, so $\tilde{\alpha}$ deviates from α. The main cause for this discrepancy is that the Bloch wave functions at k_F are strongly affected by the lattice, so it becomes increasingly inaccurate to model them as plane waves. (Of course, at very strong interactions the Hartree-Fock framework also ceases to be quantitatively accurate. However, Ref. [37] also performs a self-consistent Hartree-Fock calculation, so the discrepancy in Fig. 2 is not due to a breakdown of Hartree-Fock.)

Kane-Fisher effect in quasiperiodic systems. Having checked that our self-consistent method reproduces the Kane-Fisher effect in clean systems, we turn to quasiperiodic systems. Quasiperiodic systems have nontrivial spatial dependence of the self-consistent Hartree and exchange potentials even in the absence of an impurity. These effects renormalize the band structure and also shift the localization transition. These renormalization effects were previously studied in Refs. [15,24,44,45], and generally give rise to a mobility edge [45,46]. Intuitively, attractive interactions enhance the localization of low-energy states via self-trapping, while repulsive interactions suppress localization by screening the quasiperiodic potential. These observations are broadly consistent with our numerical results on the inverse participation ratio (IPR) as a function of disorder and energy [42].

We now explore the Kane-Fisher effect in the regime where states near the Fermi energy are clearly delocalized. Following previous studies of impurity models in quasiperiodic potentials [47,48], we work at a filling factor $f = 0.31$ at which the Fermi level lies well inside a miniband throughout the delocalized phase. We proceed exactly as above to compute the transmission coefficient, and extract a power law from its singular behavior near E_F. One subtlety that arises in the quasiperiodic case is that the tunneling depends strongly on the phase of the quasiperiodic potential. In order to isolate the effect of interactions on the transmission coefficient at any given combination of λ and θ and to facilitate the observation of the ways in which attractive and repulsive interactions renormalize the bare transmission coefficient, we tune the barrier strength to fix the bare transmission coefficient for the wave packet at the Fermi surface to the arbitrary value of 0.5 ± 0.01.

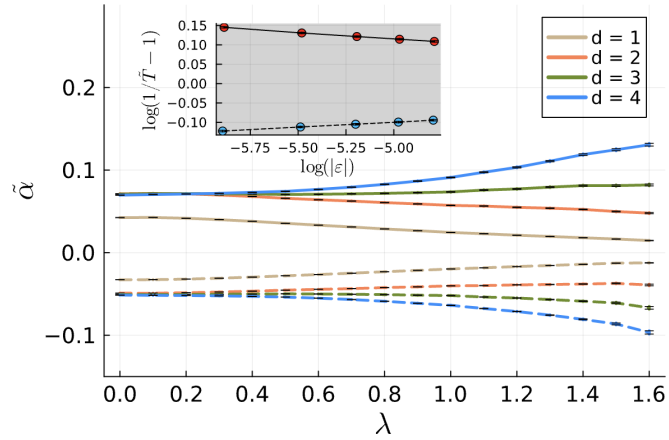

FIG. 3. Exponents $\tilde{\alpha}$ characterizing the Kane-Fisher effect in systems with increasing quasiperiodic potential strength λ. Data are computed for system size $N = 2501$, filling fraction $f = 0.31$, $v_{\text{int}} = \pm 0.6$, and averaged over 100 phase realizations. Solid lines: $\tilde{\alpha}$ from repulsive interactions; dashed lines: $\tilde{\alpha}$ from attractive interactions. Inset: Power-law relationship between ϵ and $1/\tilde{T}(\epsilon) - 1$ for system with $\lambda = 1.5$ and interaction range $d = 1$.

Our results are shown in Fig. 3. We find that for a short-ranged interaction with $d = 1$, increasing λ pushes $\tilde{\alpha}$ toward zero. Long-ranged interactions have the opposite effect, with α flowing away from zero as we increase λ. Past $\lambda \approx 1.7$, the transmission coefficient no longer behaves as a power law in $|E - E_F|$ in the energy range we are able to resolve for the available system sizes of size $\lesssim$3000 sites. This behavior is illustrated in the Supplemental Material [42].

To understand the origin of these effects, it is instructive to separate out the effects due to the Hartree and exchange interaction terms. To do this, we first solve for the self-consistent potential including both terms. Then to compute the Hartree (exchange) contribution to the transmission coefficient, we evaluate wave-packet dynamics in a quadratic Hamiltonian where the exchange (Hartree) term is artificially set to zero. From this we again extract an exponent, which we call the Hartree (exchange) exponent (Fig. 4). The exchange exponent behaves as one would expect, growing stronger with increasing λ as the bands grow flatter. The behavior of the Hartree term is more subtle. At filling fraction 0.31, the Bloch states are rather far from continuum plane waves, so the Hartree term is not well described by simply taking the Fourier transform of the interaction potential. In the clean limit, at this filling, we find that the Hartree and exchange terms in fact have the same sign. Upon increasing λ, the sign of the Hartree effect flips. The strength of this term is also nonmonotonic with interaction range: For long-range interactions the term is increasingly suppressed, as one would expect (a smoothly varying potential has no effect on scattering). However, for

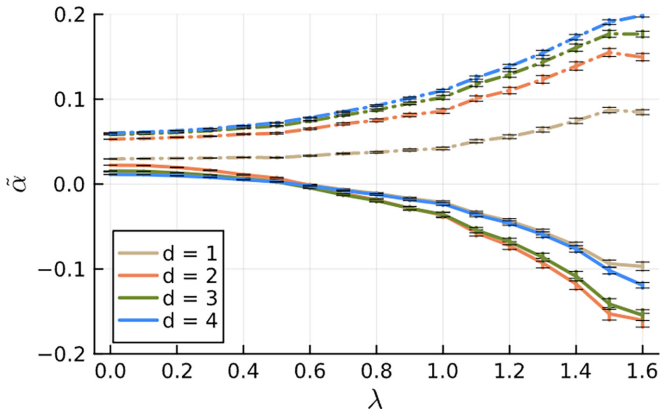

FIG. 4. Hartree (exchange) exponents $\tilde{\alpha}$ characterizing the Hartree (exchange) contribution to the Kane-Fisher effect in systems with increasing quasiperiodic potential strength λ. Data are computed for system size $N = 2501$, filling fraction $f = 0.31$, repulsive interaction $v_{\text{int}} = 0.6$, and averaged over 100 phase realizations. Solid lines: Hartree exponent. Dashed-dotted lines: Exchange exponent.

short-range potentials, the Hartree term becomes increasingly strong and negative as λ is increased. This is the origin of the suppression of interaction effects: As remarked in the introduction, the interactions projected onto the miniband at the Fermi level are increasingly contactlike as the minibands become sparser, so the Hartree and Fock terms cancel as they would for contact interactions.

Discussion. This Letter explored how Luttinger-liquid behavior emerges in the low-energy limit of interacting quasiperiodic systems. We found clear evidence by two different methods that Luttinger-liquid behavior does emerge, albeit with a strongly renormalized Luttinger parameter. The Luttinger parameter exhibits a counterintuitive dependence on the strength of the quasiperiodic potential λ: For short-range interactions, as λ is tuned toward the localization transition, the Luttinger parameter approaches that of the free system, although the bands get very flat. We identified the origin of this phenomenon as a cancellation between Hartree and Fock terms that becomes more pronounced at larger λ. This cancellation occurs because the characteristic spatial scale of the miniband at the Fermi level grows (with correlation length $\xi \sim 1/|\lambda_c - \lambda|$) with increasing λ.

Our conclusions are consistent with (and complementary to) those found by Ref. [31] exploring interaction effects at the Aubry-André critical point: While that work focuses on the critical point itself, we show how this regime emerges coming from the Luttinger liquid. Reference [31] concluded, based on a scaling argument, that finite-range interactions are always irrelevant at the Aubry-André critical point. This would imply that the curves in Fig. 3 are in fact nonmonotonic: Very close to the transition, we expect the effective Luttinger parameter to dip again toward $K = 1$. We do not see this numerically, and there are at least two plausible explanations for why. The first is that the Luttinger parameter eventually dips back down, but in a parameter regime where we are unable to see a clean Kane-Fisher effect. A second possibility is that at finite (as opposed to infinitesimal) interaction strengths, interactions renormalize the localization problem sufficiently to alter the nature of the Aubry-André transition (e.g., the fractal structure of energy levels). This second possibility is less exotic than it sounds. If one considers a two-dimensional phase diagram with interaction strength and quasiperiodicity as the axes, the critical behavior found in Ref. [31] must change to the behavior found using Luttinger-liquid theory [23] somewhere along the phase boundary, and it is natural for this location to depend on the interaction range. Exploring this question in more detail, and developing a complete theory of this unusual critical phenomenon, is an interesting challenge for future work.

The framework we have used also naturally extends to two-dimensional systems. Quasiperiodic systems in higher dimensions (which are relevant to moiré materials [17,49]) exhibit a richer phase diagram at the noninteracting level, with ballistic, diffusive, and localized phases [50,51]. The analog of the Kane-Fisher effect in two dimensions is the Altshuler-Aronov suppression of the density of states [52], which can again be understood in terms of renormalized Friedel oscillations. It would be interesting to explore these effects in the quasiperiodic case. In particular, our results would suggest that the cancellation between Hartree and Fock terms would also suppress the effects of short-range interactions in these two-dimensional systems.

Acknowledgments. We thank David Huse and Jed Pixley for useful conversations. This work was supported by NSF Grants No. DMR-2103938 (T.J.V., S.G.) and No. DMR-2104141 (R.V.).

[1] M. Imada, A. Fujimori, and Y. Tokura, Metal-insulator transitions, Rev. Mod. Phys. **70**, 1039 (1998).

[2] L. Sanchez-Palencia and M. Lewenstein, Disordered quantum gases under control, Nat. Phys. **6**, 87 (2010).

[3] T. Vojta, Disorder in quantum many-body systems, Annu. Rev. Condens. Matter Phys. **10**, 233 (2019).

[4] A. Kapitulnik, S. A. Kivelson, and B. Spivak, *Colloquium:* Anomalous metals: Failed superconductors, Rev. Mod. Phys. **91**, 011002 (2019).

[5] T. Giamarchi and H. J. Schulz, Anderson localization and interactions in one-dimensional metals, Phys. Rev. B **37**, 325 (1988).

[6] E. Altman, Y. Kafri, A. Polkovnikov, and G. Refael, Insulating phases and superfluid-insulator transition of disordered boson chains, Phys. Rev. Lett. **100**, 170402 (2008).

[7] L. Pollet, N. V. Prokof'ev, B. V. Svistunov, and M. Troyer, Absence of a direct superfluid to Mott insulator transition in disordered Bose systems, Phys. Rev. Lett. **103**, 140402 (2009).

[8] L. Pollet, N. V. Prokof'ev, and B. V. Svistunov, Asymptotically exact scenario of strong-disorder criticality in one-dimensional superfluids, Phys. Rev. B **89**, 054204 (2014).

[9] E. V. H. Doggen, G. Lemarié, S. Capponi, and N. Laflorencie, Weak- versus strong-disorder superfluid—Bose glass transition in one dimension, Phys. Rev. B **96**, 180202(R) (2017).

[10] G. Roati, C. D'Errico, L. Fallani, M. Fattori, C. Fort, M. Zaccanti, G. Modugno, M. Modugno, and M. Inguscio, Anderson localization of a non-interacting Bose–Einstein condensate, Nature (London) **453**, 895 (2008).

[11] M. Schreiber, S. S. Hodgman, P. Bordia, H. P. Lüschen, M. H. Fischer, R. Vosk, E. Altman, U. Schneider, and I. Bloch, Observation of many-body localization of interacting fermions in a quasirandom optical lattice, Science **349**, 842 (2015).

[12] M. Sbroscia, K. Viebahn, E. Carter, J.-C. Yu, A. Gaunt, and U. Schneider, Observing localization in a 2D quasicrystalline optical lattice, Phys. Rev. Lett. **125**, 200604 (2020).

[13] H. P. Lüschen, P. Bordia, S. Scherg, F. Alet, E. Altman, U. Schneider, and I. Bloch, Observation of slow dynamics near the many-body localization transition in one-dimensional quasiperiodic systems, Phys. Rev. Lett. **119**, 260401 (2017).

[14] H. P. Lüschen, S. Scherg, T. Kohlert, M. Schreiber, P. Bordia, X. Li, S. Das Sarma, and I. Bloch, Single-particle mobility edge in a one-dimensional quasiperiodic optical lattice, Phys. Rev. Lett. **120**, 160404 (2018).

[15] F. A. An, K. Padavić, E. J. Meier, S. Hegde, S. Ganeshan, J. H. Pixley, S. Vishveshwara, and B. Gadway, Interactions and mobility edges: Observing the generalized Aubry-André model, Phys. Rev. Lett. **126**, 040603 (2021).

[16] K. F. Mak and J. Shan, Semiconductor moiré materials, Nat. Nanotechnol. **17**, 686 (2022).

[17] Y. Fu, E. J. König, J. H. Wilson, Y.-Z. Chou, and J. H. Pixley, Magic-angle semimetals, npj Quantum Mater. **5**, 71 (2020).

[18] A. Chandran and C. R. Laumann, Localization and symmetry breaking in the quantum quasiperiodic Ising glass, Phys. Rev. X **7**, 031061 (2017).

[19] P. J. D. Crowley, A. Chandran, and C. R. Laumann, Quasiperiodic quantum Ising transitions in 1D, Phys. Rev. Lett. **120**, 175702 (2018).

[20] P. J. D. Crowley, C. R. Laumann, and A. Chandran, Critical behavior of the quasi-periodic quantum Ising chain, J. Stat. Mech. (2022) 083102.

[21] P. J. D. Crowley, C. R. Laumann, and S. Gopalakrishnan, Quantum criticality in Ising chains with random hyperuniform couplings, Phys. Rev. B **100**, 134206 (2019).

[22] J. Vidal, D. Mouhanna, and T. Giamarchi, Correlated fermions in a one-dimensional quasiperiodic potential, Phys. Rev. Lett. **83**, 3908 (1999).

[23] G. Roux, T. Barthel, I. P. McCulloch, C. Kollath, U. Schollwöck, and T. Giamarchi, Quasiperiodic Bose-Hubbard model and localization in one-dimensional cold atomic gases, Phys. Rev. A **78**, 023628 (2008).

[24] V. Mastropietro, Localization of interacting fermions in the Aubry-André model, Phys. Rev. Lett. **115**, 180401 (2015).

[25] P. Naldesi, E. Ercolessi, and T. Roscilde, Detecting a many-body mobility edge with quantum quenches, SciPost Phys. **1**, 010 (2016).

[26] T. Cookmeyer, J. Motruk, and J. E. Moore, Critical properties of the ground-state localization-delocalization transition in the many-particle Aubry-André model, Phys. Rev. B **101**, 174203 (2020).

[27] U. Agrawal, S. Gopalakrishnan, and R. Vasseur, Universality and quantum criticality in quasiperiodic spin chains, Nat. Commun. **11**, 2225 (2020).

[28] C. Schuster, R. A. Römer, and M. Schreiber, Interacting particles at a metal-insulator transition, Phys. Rev. B **65**, 115114 (2002).

[29] Y. E. Kraus, O. Zilberberg, and R. Berkovits, Enhanced compressibility due to repulsive interaction in the Harper model, Phys. Rev. B **89**, 161106(R) (2014).

[30] D. Vu and S. Das Sarma, Moiré versus Mott: Incommensuration and interaction in one-dimensional bichromatic lattices, Phys. Rev. Lett. **126**, 036803 (2021).

[31] M. Gonçalves, J. H. Pixley, B. Amorim, E. V. Castro, and P. Ribeiro, Short-range interactions are irrelevant at the quasiperiodicity-driven Luttinger liquid to Anderson glass transition, Phys. Rev. B **109**, 014211 (2024).

[32] Y. Yoo, J. Lee, and B. Swingle, Nonequilibrium steady state phases of the interacting Aubry-André-Harper model, Phys. Rev. B **102**, 195142 (2020).

[33] R. Chi, J. J. Yu, C. Murthy, and T. Xiang, Luttinger liquid phase in the Aubry-André Hubbard chain, arXiv:2401.08980.

[34] H. Hiramoto and M. Kohmoto, Scaling analysis of quasiperiodic systems: Generalized Harper model, Phys. Rev. B **40**, 8225 (1989).

[35] S. R. White, Density matrix formulation for quantum renormalization groups, Phys. Rev. Lett. **69**, 2863 (1992).

[36] U. Schöllwock, The density-matrix renormalization group in the age of matrix product states, Ann. Phys. **326**, 96 (2011).

[37] D. Yue, L. I. Glazman, and K. A. Matveev, Conduction of a weakly interacting one-dimensional electron gas through a single barrier, Phys. Rev. B **49**, 1966 (1994).

[38] M. Wilkinson, Critical properties of electron eigenstates in incommensurate systems, Proc. R. Soc. Lond. A **391**, 305 (1984).

[39] M. Kohmoto, B. Sutherland, and C. Tang, Critical wave functions and a Cantor-set spectrum of a one-dimensional quasicrystal model, Phys. Rev. B **35**, 1020 (1987).

[40] M. P. Zaletel, R. S. K. Mong, C. Karrasch, J. E. Moore, and F. Pollmann, Time-evolving a matrix product state with long-ranged interactions, Phys. Rev. B **91**, 165112 (2015).

[41] T. Giamarchi, *Quantum Physics in One Dimension* (Clarendon Press, Oxford, UK, 2003), Vol. 121.

[42] See Supplemental Material at http://link.aps.org/supplemental/10.1103/PhysRevB.110.L020201 for data on localization lengths and further numerical support for the main claims.

[43] C. L. Kane and M. P. A. Fisher, Transport in a one-channel Luttinger liquid, Phys. Rev. Lett. **68**, 1220 (1992).

[44] A. Štrkalj, E. V. H. Doggen, I. V. Gornyi, and O. Zilberberg, Many-body localization in the interpolating Aubry-André-Fibonacci model, Phys. Rev. Res. **3**, 033257 (2021).

[45] Y. Wang, J.-H. Zhang, Y. Li, J. Wu, W. Liu, F. Mei, Y. Hu, L. Xiao, J. Ma, C. Chin, and S. Jia, Observation of interaction-induced mobility edge in an atomic Aubry-André wire, Phys. Rev. Lett. **129**, 103401 (2022).

[46] J. Biddle, B. Wang, D. J. Priour, and S. Das Sarma, Localization in one-dimensional incommensurate lattices beyond the Aubry-André model, Phys. Rev. A **80**, 021603(R) (2009).

[47] A.-K. Wu, S. Gopalakrishnan, and J. H. Pixley, Fractal x-ray edge problem at the critical point of the Aubry-André model, Phys. Rev. B **100**, 165116 (2019).

[48] A.-K. Wu, D. Bauernfeind, X. Cao, S. Gopalakrishnan, K. Ingersent, and J. H. Pixley, Aubry-André Anderson model: Magnetic impurities coupled to a fractal spectrum, Phys. Rev. B **106**, 165123 (2022).

[49] J. H. Pixley, J. H. Wilson, D. A. Huse, and S. Gopalakrishnan, Weyl semimetal to metal phase transitions driven by quasiperiodic potentials, Phys. Rev. Lett. **120**, 207604 (2018).

[50] T. Devakul and D. A Huse, Anderson localization transitions with and without random potentials, Phys. Rev. B **96**, 214201 (2017).

[51] A. Szabó and U. Schneider, Mixed spectra and partially extended states in a two-dimensional quasiperiodic model, Phys. Rev. B **101**, 014205 (2020).

[52] B. L. Altshuler, A. G. Aronov, and P. A. Lee, Interaction effects in disordered Fermi systems in two dimensions, Phys. Rev. Lett. **44**, 1288 (1980).